4 MODEL DEVELOPMENT

4.1 Microsim and model requirements

The Microsim unit library contains general models of most ore dressing unit operations. However, the plant we wish to simulate contains a gyradisc crusher for which no model exists. The existing screening models do not allow for the use of poly decks and non-square screen apertures, both of which are used on the plant. Furthermore, the ore to be treated is particularly hard and the generalised constants employed in the existing Whiten crushing model are inappropriate.

The following four models were thus incorporated into Microsim, to cater for the requirements of this plant:

a modified Whiten crushing model, programmed as overlay procedure CRUSH6_7, a semi-empirical model for crushing haematite

a new empirical Gyradisc crushing model, programmed as overlay procedure CRUSH5

an enhanced Karra screen model, programmed as overlay procedure SCREEN5, an empirical model for poly decks with non-square apertures

new Rose efficiency models, programmed as overlay procedures ROSE1 and ROSE2, using experimentally determined screening efficiencies.

All other unit models remain in the unit library, although the original Whiten model was deleted because of the limit on number of models per unit type. The Pascal listings for these models can be found in Appendix 3.

For the purpose of model development, crushing was considered homogeneous (i.e. crushing characteristics did not vary with grade) and screening was likewise considered uniform for all grades of material.

Microsim requires that models developed are programmed in a particular way (as outlined below) to fit the sequential modular

All models must have as input only one stream, and as output as many streams as are given by the icon for the unit type. For crushers, only one output stream is permitted, single deck screens have two and double deck screens have three output streams.

Each model has as input the complete feed stream array, and mass flow rate of the stream, together with model parameters. The model can also access system data (e.g. specific gravity of pure components).

The solution to each model is required to be the complete specification of the mass flow rates and stream arrays for each output stream. Thus the model must manipulate the input data according to given equations to give a solution of this form.

The models will be accessed as many times as determined by the ordering program. Upon completion of a simulation, the user may request graphical or tabular output of mass flow rates, size and grade distributions and/or partition curves, as appropriate.

The complete Pascal overlay procedures were inserted into the unit library (UNIT1.PAS for crushing models and UNIT2.PAS for screening models). The CASE statements in MODELS.PAS for crushers, single deck screens and double deck screens were updated, and the file OVERLAY.PAS was compiled to create a file SIMULATE.COM. The new model names were entered in the data file MODEL.DAT. The program DBASE was run to enter new model parameters as well as default values for these parameters. It is necessary to incorporate text for relevant questions into the database using this program. These questions (and default values) will then be displayed on the screen prompting the user to enter required data for a given flowsheet.

Microsim is now ready to be used as outlined in chapter 3.

4.2 Crushing models

4.2.1 Whiten model

The Whiten model (see section 3.3 for the theory) as written in Microsim was not suitable for use in its original form as the breakage characteristics were average values rather than those of a specific ore and crushing application.

The model parameters which must be entered by the user are the closed side setting, CSS, in metres, the fractional proportion of fines produced during breakage events, K, and the impact work index, IWI, in kWh/t. The impact work index for the iron ore is 26,4kWh/t. The value of K was found to be dependent on the breakage events occurring in the crusher.

The model has a breakage function with exponents m and n. These exponents are ore-specific. Whiten (57) has documented the values of exponents m and n for haematite. The value of m is given as 0,535. This value is close to the generalised value used in the original Microsim model of 0,5. The value of n is related to the number of breakage events in the crusher. For both Nordberg Symons cone crushers and shorthead crushers five breakage events occur. From the work of Whiten (57) on haematite it was found that this corresponded to a value for n of 2,0 (cf. 4,5 for the existing Microsim model) and an average value for K of 0,2. The parameter K depends on CSS and to a lesser degree on the feed rate to the crusher.

The algorithm for procedure CRUSH6_7 is as follows:

(1) determine total flow rate in each size class in the input stream

(2) from the smallest size class to the largest:

(2.1) calculate amount of material of size x classified from the classification function

$$c=1-\left((x-k2)/(k1-k2) \right)^{k3}$$

where k1=0,653CSS for Symons crushers
k1=0,944CSS for shorthead crushers
k2=1,21CSS for Symons crushers

k2=1,722CSS+0,004826 for shorthead crushers

k3=2,0 for Symons crushers

k3=3,0 for shorthead crushers

and multiply by the mass in the class, then assign this material to output stream

(2.2) for this class and smaller classes, calculate the mass breakage from P, the fraction of material of size less than x produced by breakage of particles of size y

$$P=(1-K)(x/y)^n+K(x/y)^m$$

and multiply by the mass in the classes, then assign masses to output stream

(2.3) increase size class by 1 and return to 2.1

(3) exit model with stream array completed.

The model is suitable for use where the feed rate is within the manufacturers' specifications:

Symons 7ft crusher:	330-1250 tph	-460mm feed
Symons 10ft crusher:	400-1400 tph	-660mm feed
Shorthead 7ft crusher:	109-500 tph	-210mm feed.

The model does not take into account variation in feed rate, although it has been stated that the parameter K is weakly dependent on feed rate, which is not known *a priori*. This dependence was thought small enough to be neglected. It is left to the user to enter a value of K corresponding to the input CSS. The user should also check the output of the simulator to confirm that the flow rate through the crusher is within design specification.

4.2.3 Gyradisc model

An empirical model for crushing in a gyradisc crusher was developed largely from manufacturers' data, with consideration of the theory of crushing.

Material fed to a gyradisc crusher is distributed around the crushing chamber where it undergoes interparticle comminution, and is moved towards the discharge by the rotation of the crusher spindle. As the liners are set at an angle less than the angle of repose of the material, it is this motion which determines the residence time of material in the crusher. Particles within the crusher can undergo interparticle comminution in two ways. They can be compressed by other particles and undergo compressive breakage, or they can be abraded by friction as other particles move relative to them.

Since a gyradisc crusher is used for fine material, it is expected that the approximation to the Griffith crack theory for fine particles (29) will be valid. This approximate theory states that the size distribution of fracture products resulting from each fracture mechanism can be expressed by a Rosin-Rammler equation. Since we have two fracture mechanisms, we anticipate two Rosin-Rammler distributions. A similar argument was used for larger crushers where the two fracture mechanisms were compressive and tensile breakage.

Product size distributions obtained from the Gyradisc Crusher Manual (39) for a variety of crushing applications were plotted on RR plots and two distributions were indeed found, one for finer material and a steeper one for coarser material. Figures 15 and 16 are examples of two such plots, one for crushing trap rock, also a hard material, and the other for crushing haematite.

Since particles larger than the CSS will undergo compressive failure, we hypothesise that the upper distribution represents the products formed from compressive failure and that the lower distribution represents those formed by abrasion.

It is known that the product from a gyradisc crusher coarsens with increasing CSS. The dependence of the product size distribution was assumed to be linear. For this reason the particle size used in figure 16 has been non-dimensionalised using the CSS.

From figure 16, the product size distribution can be characterised from the slopes and intercepts of the two RR plots.

The fine distribution has a (non-dimensional) reference size, k, of 250 and an exponent, n, of 0,32 whereas the coarse distribution has a reference size, k, of 0,38 and an exponent, n, of 2,77. The two

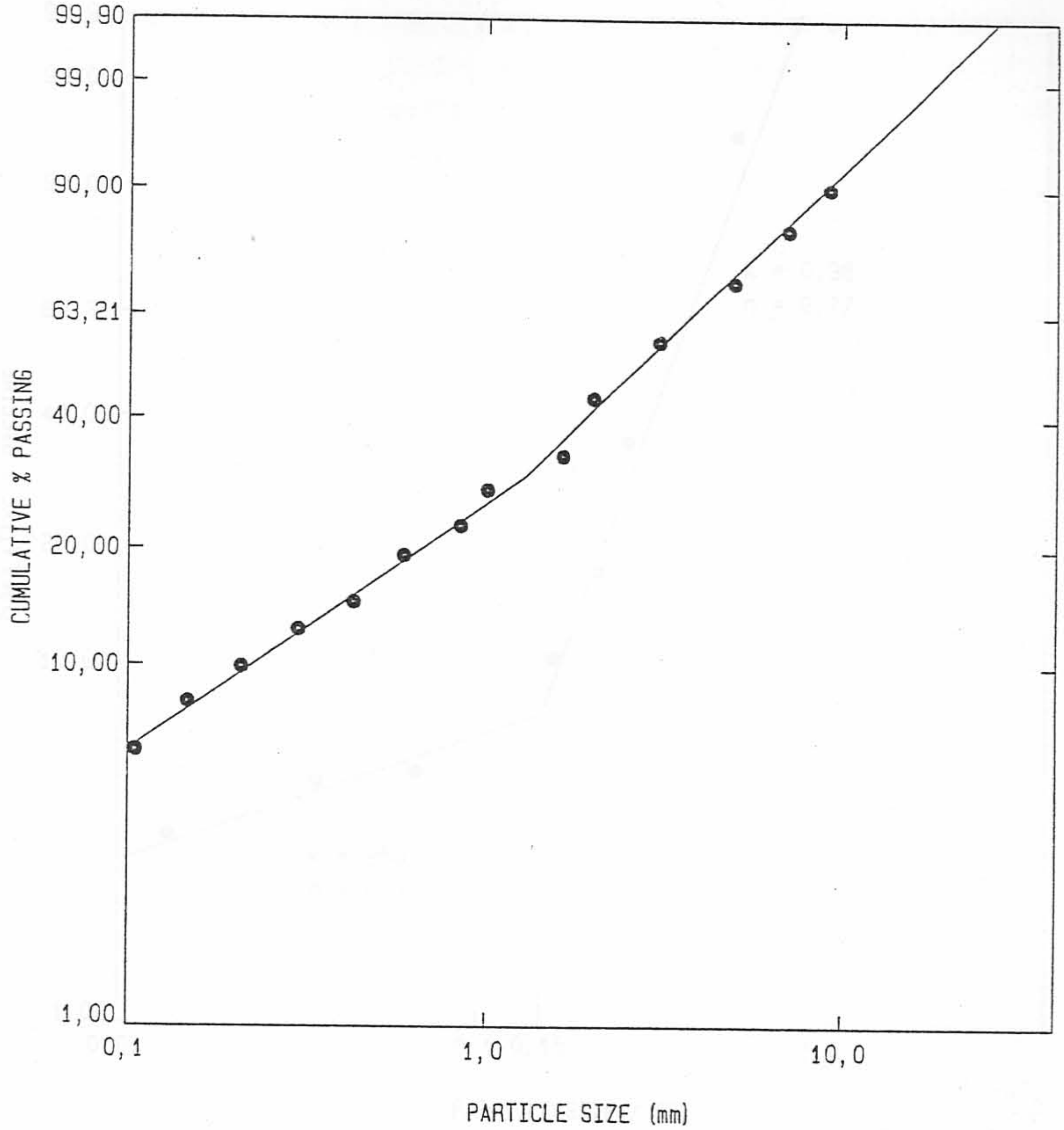

Fig 15 Rosin-Rammler plot for output from gyradisc crushing trap rock

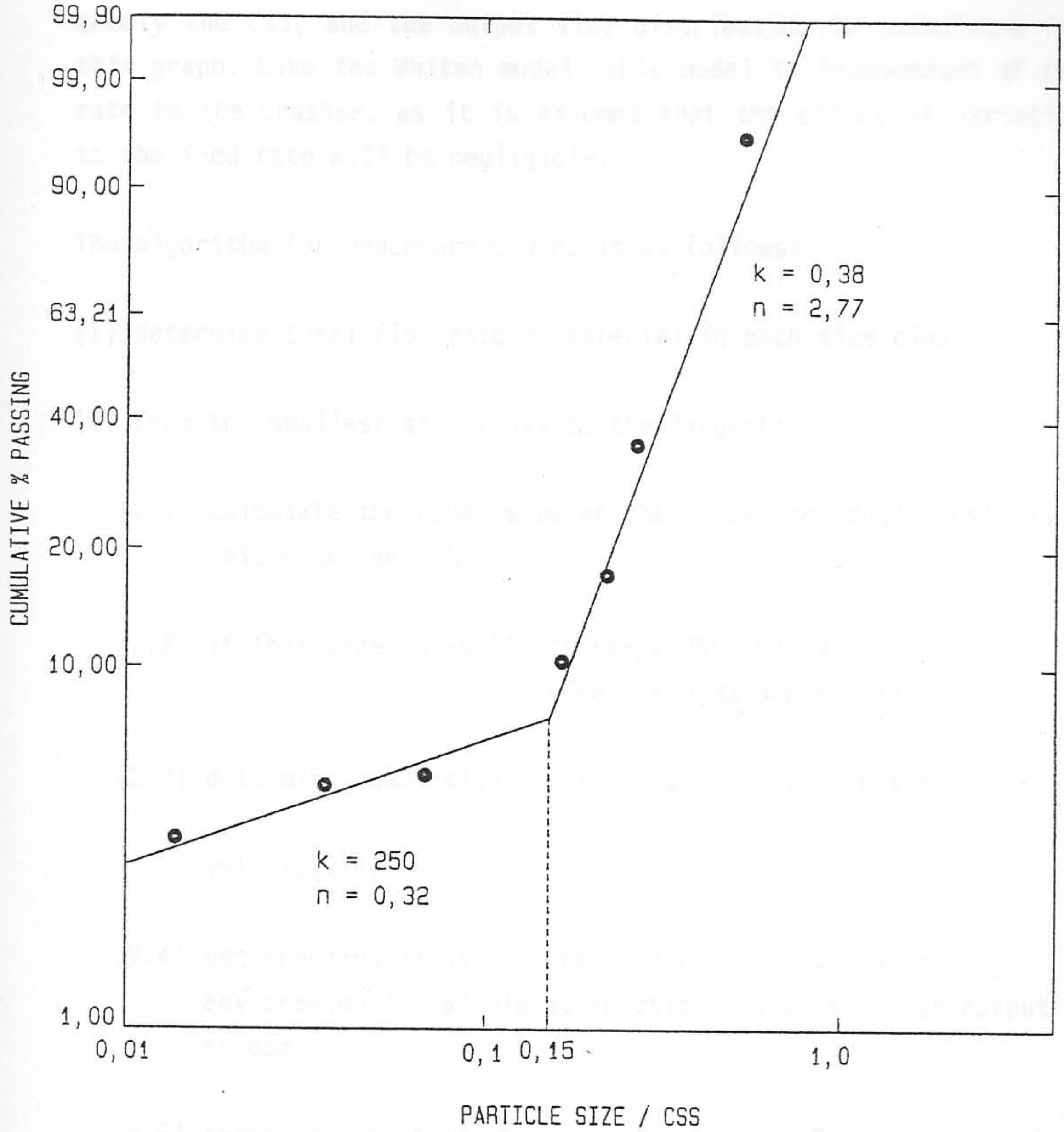

Fig 16 Rosin-Rammler plot for output from gyradisc crushing iron ore

distributions intersect at a non-dimensional particle size of 0,15.

This graph gives an output size distribution dependent only on CSS. Therefore the computer model was written with only one parameter, namely the CSS, and the output size distribution is calculated from this graph. Like the Whiten model, this model is independent of feed rate to the crusher, as it is assumed that the effect of variations to the feed rate will be negligible.

The algorithm for procedure CRUSH5 is as follows:

(1) determine total flow rate of material in each size class

(2) from the smallest size class to the largest:

(2.1) calculate the upper size of the class and non-dimensionalise this with the CSS

(2.2) if this size is <0,15, choose k=250 and n=0,32
else k=0,38 and n=2,77

(2.3) determine cumulative fraction passing, y, for size x

$y=1-\exp(x/k)^n$

(2.4) get fraction passing in this size class by subtracting any previously calculated fractions, and assign to output stream

(2.5) increase size class by one and return to 2.1.

(3) exit the model with stream array complete

The model is only valid for flow rates within the maufacturers' specified capacity of 250-300tph of -38mm material. The top size of the feed should be greater that four-fifths of the CSS. This model should not be used to predict the product size distribution of a crusher that is choke fed as this could entrap particles and lead to a greater fraction of fine material being produced.

4.3 Screening models

4.3.1 Enhanced Karra model

The Karra model, the theory of which was given in section 3.4, was modified to take into account the effect of poly decks and of non-square apertures in the following way.

If a poly deck is used, the effective screen area is less than that of an equivalent wire deck. From poly decks presently used on the plant, the average reduction was determined to be 15%. This is also the value used in the empirical Ateliers Bergeaud Macon model, which was supplied by Nordberg (38).

A shape factor was used to account for the non-square aperture effect on screening efficiency. The value of the shape factor, H, for aperture length, l, and width, w, was obtained from Kelly & Spottiswood (29) as:

H = 1,0 for l/w ratio up to 2
H = 1,1 for l/w ratio from 2 to 3
H = 1,4 for l/w ratio from 3 to 6
H = 1,6 for l/w ratio above 6

The model requires six parameters for single deck screening, and ten parameters for double deck screening:

total screen area
angle of inclination of the screen
aperture width, top deck
aperture length, top deck
wire (or poly) thickness, top deck
poly or wire, top deck
aperture width, bottom deck
aperture length, bottom deck
wire (or poly) thickness, bottom deck
poly or wire, bottom deck.

The algorithm for the procedure SCREEN5 is as follows:

(1) from input data determine the empirical coefficients A to H: (the correlations for these factors are given in Appendix 2)

A=basic capacity factor

B=percentage oversize in feed factor

C=percentage halfsize in feed factor

D=deck location factor

E=wet screening factor

F=bulk density of material

G=reduced area coefficient (1/1,15 for poly deck)

H=shape factor (given above)

and calculate theoretical undersize flow rate (T), screen area (S) and % near size in feed (L)

(2) calculate Z=T/S/(ABCDEFGH)

(3) calculate efficiency=$0{,}975Z^{-0{,}148}(1-L/100)^{0{,}511}$

(4) calculate d50=efficiency(throughfall aperture)

(5) from the smallest size class to the largest:

(5.1) calculate partition coefficients, c, of each deck at the representative size, x. If this size is greater than the aperture size set the partition coefficient equal to 1

$$c=1-\exp(-0{,}693(x/d50)^{5{,}846})$$

(5.2) for top deck apportion the mass in the size class to the over- and underflow according to the partition coefficient

(5.3) using the top deck underflow and the bottom deck partition coefficient, apportion the overflow and underflow of this deck

(5.4) increase the size class by 1 and return to 5.1

(6) exit the procedure with the completed output stream arrays.

This model should only be used within the capacity range 17-53tph per square metre of screen area. It is also limited to screening crushed rock and ores.

4.3.2 Rose efficiency model

The Rose test and model described in section 3.4 determine an equilibrium efficiency for a given screen. This efficiency is determined from the values of the blinding, unblinding and screen passage rates. In the plant the equilibrium efficiencies of various screens are known from operating data gathered in many conditions over the years of operation.

The model was developed using this global equilibrium efficiency as one parameter, the other parameter being the screen size at which this efficiency was obtained. This efficiency is then used to calculate d50, equal to the undersize efficiency multiplied by the throughfall aperture. This is identical to Karra's method of calculating the d50 once a screening efficiency is known and is a very good approximation when efficiencies are between 0,7 and 0,95. All efficiencies recorded for the plant are within this range.

Once the d50 has been calculated, the partition curve of the form recommended by Ford (16) and used by Karra (see section 3.4) was used to determine the size distributions in the product streams.

This model has separate versions for both single deck and double deck screening, incorporated in the Microsim library as overlay procedures ROSE1 and ROSE2 respectively.

The model has the following parameters:

screen aperture for top deck on which efficiency is based
efficiency for top deck
screen aperture for bottom deck on which efficiency is based
efficiency for bottom deck

The algorithm for double deck screening is as follows:

(1) calculate the d50 of each deck from the respective screen apertures and the efficiencies

(2) from the smallest size class to the largest:

(2.1) calculate the partition coefficients, c, of each deck at the representative size, x. If this size is greater than the aperture size set the partition coefficient equal to 1

$$c=1-\exp(-0{,}693(x/d50)^{5{,}846})$$

(2.2) for the top deck apportion the mass in the size class to the over- and underflow according to the partition coefficient

(2.3) using the top deck underflow and the bottom deck partition coefficient, apportion the overflow and underflow of this deck

(2.4) increase the size class by 1 and return to 2.1

(3) exit the procedure with the completed output stream arrays.

This model does not incorporate the effect of variations in the feed rate to the screen. Variations in feed rate alter the vibration characteristics of the screen and the bed depth by altering the load on the screen. The change in bed depth will alter the segregation of particles on the screen. It is thus difficult to quantify the effect of variations in feed rate. A rule of thumb exists (29) that states that the screening efficiency varies linearly with feed rate. If an efficiency of 80% represents 100% feed rate, efficiency will decrease by a quarter of a percent for each percent increase in feed up to 140%, and will increase by a quarter of a percent for each percent decrease in feed below 100%, down to about 60%.

It is the responsibility of the user to check the feed rate to the screen after a simulation and to modify the screening efficiency if the flow rate deviates markedly from the rate at which the efficiency was determined. It is expected from the user to ascertain that the feed size distribution does not cause screening efficiencies to change significantly.

5 MODEL VALIDATION AND DISCUSSION

In this chapter, models are tested individually against each other and experimental data. In chapter 6 on plant simulation, models are used in various combinations and at various operating conditions, and compared with plant data.

5.1 Crushing models

The crushing models were tested using a very simple flowsheet in Microsim as given in figure 17.

5.1.1 Whiten model

Whiten's model has been improved to include the correct parameters for the iron ore and the number of breakage events occurring in the crushers on this plant. This is a more appropriate version of the original model in the Microsim unit model library for this application. For use on other plants it will have to be modified again to include the relevant parameters for that plant.

The model caters for both standard Symons cone crushers, as used on the plant for secondary and tertiary crushing, and shorthead crushers, as used in the quaternary plant.

The model was tested for Symons crushers using data collected from the tertiary crusher, operating at a flow rate of approximately 600tph. The CSS was 50mm, and the values of K and IWI required by the model were taken as 0,2 and 26,4kWh/t. Figure 18 gives the output size distribution of the Whiten model, together with experimental values and that of the Nordberg model in the Microsim unit library.

It can be seen that the Whiten model gives a more accurate output size distribution than does the Nordberg model, and that the Whiten model agrees closely with experimental values.

For shorthead crushers, the model was tested using data collected from the fresh feed crusher of the quaternary plant. The CSS was 25mm, and feed rate 520tph and the values of K and IWI were taken as 0,2 and 26,4kWh/t respectively. Figure 19 gives the output size distribution predicted by the Whiten model for a shorthead crusher

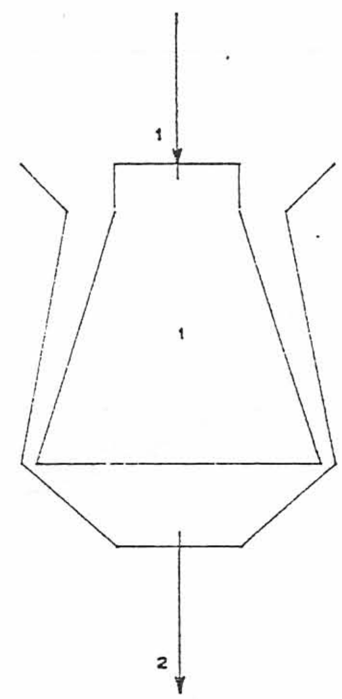

Fig 17 Flowsheet for testing crusher models

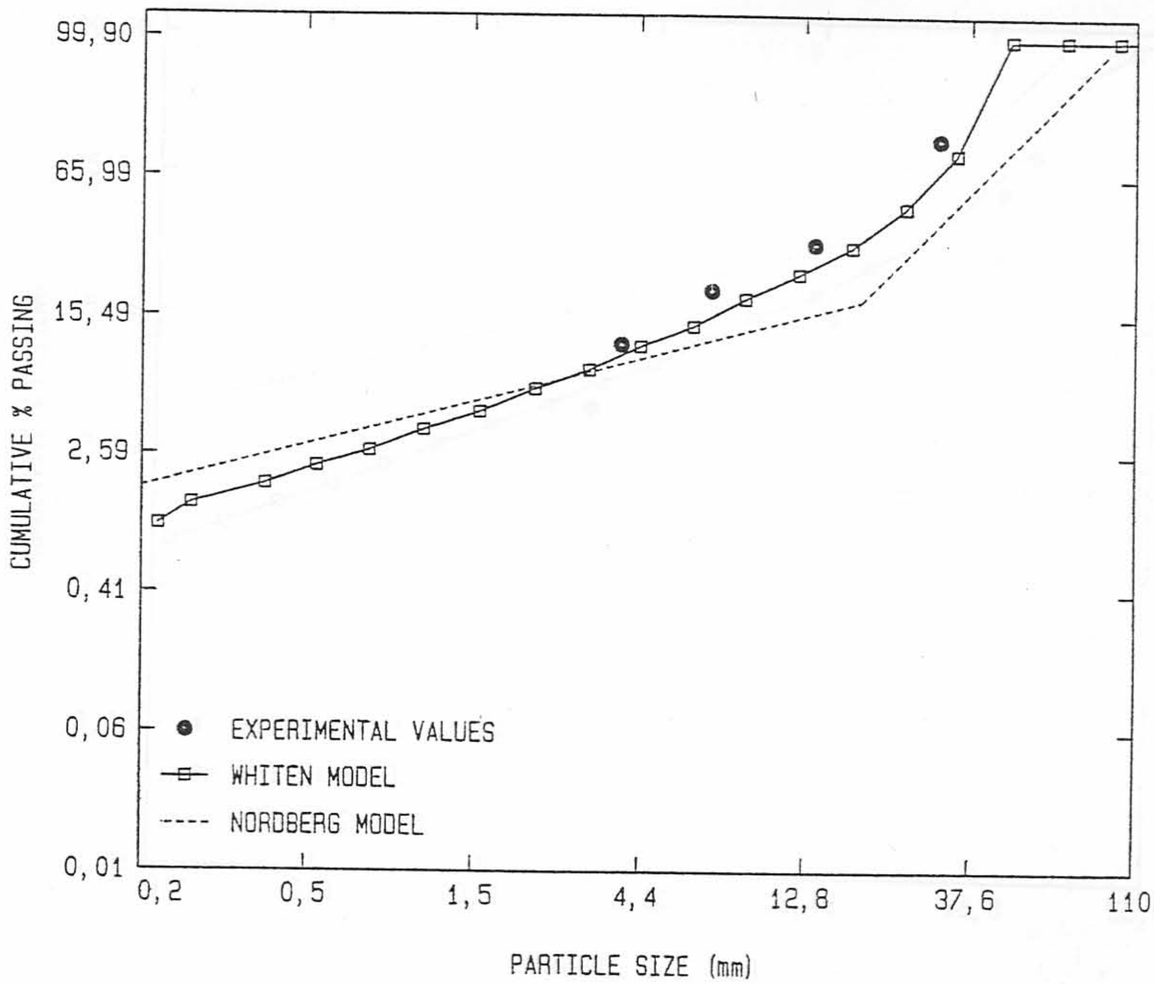

Fig 18 Rosin-Rammler plot for Whiten and Nordberg models output with closed side setting of 50mm, and experimental values

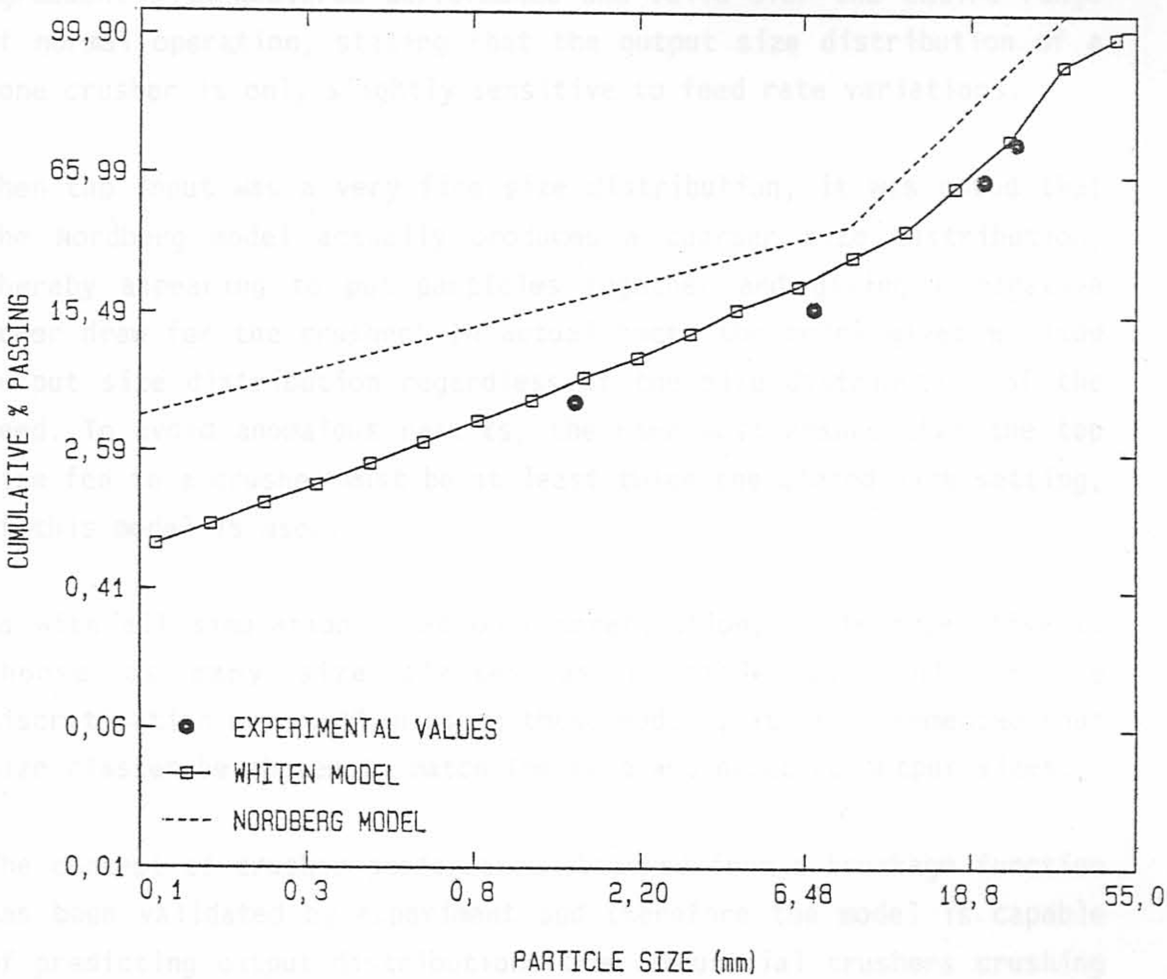

Fig 19 Rosin-Rammler plot for Whiten and Nordberg models output with closed side setting of 25mm, and experimental values

for a closed side setting of 25mm, together with experimental values and values predicted by the Nordberg model.

The Whiten model again gives a more accurate prediction than the Nordberg model and agrees closely with experimental values.

Whiten (57) has also used this model with the parameters as specified for haematite (and incorporated in the new model) on an Australian crushing application and found it to be in excellent agreement with measured performance and valid over the entire range of normal operation, stating that the output size distribution of a cone crusher is only slightly sensitive to feed rate variations.

When the input was a very fine size distribution, it was noted that the Nordberg model actually produces a coarser size distribution, thereby appearing to put particles together and giving a negative power draw for the crusher! In actual fact, the model gives a fixed output size distribution regardless of the size distribution of the feed. To avoid anomalous results, the user must ensure that the top size fed to a crusher must be at least twice the closed side setting, if this model is used.

As with all simulation based on discretisation, it is imperative to choose as many size classes as possible to minimise the discretisation error. When using these models, it is recommended that size classes be chosen to match the feed and expected output sizes.

The concept of crusher performance obtained from a breakage function has been validated by experiment and therefore the model is capable of predicting output distributions from industrial crushers crushing haemetite. For greater accuracy the dependence of K, the proportion of fines produced during breakage events, on the CSS, should be experimentally established.

5.1.2 Gyradisc model

This new gyradisc model was tested against data obtained from separate test runs on the gyradisc crusher of the quaternary plant.

For various values of closed side setting (the dependent variable in the gyradisc model), feed and product size distributions were determined by screen analysis of a belt cut. From the given input size distributions the model was run and the product size distributions were compared with those determined by screening analysis. Figures 20 to 23 give these comparisons with experimental values.

For figure 20, CSS=20mm, feed rate = 200tph
figure 21, CSS=17mm, feed rate = 280tph
figure 22, CSS=14mm, feed rate = 210tph
figure 23, CSS=13mm, feed rate = 350tph.

The gryadisc model shows very good agreement with experimentally measured data for a variety of closed side settings. The measurements were taken over a wide range of flow rates (even outside the manufacturers' specifications of 250-300tph) and the results appear to be insensitive to a change in flowrate.

Thus the gyradisc model very accurately predicts the product size distribution from the crusher and validates the use of CSS as the only model parameter. The model can also be used for a wider range of feed rates than the manufacturers specify.

This model can be used for closed side settings of up to 25mm, and the feed must be -38mm, with a top size of above 0,8CSS.

It is expected that the parameters of the fine and coarse size distributions will vary according to ore type. The model is therefore only valid for haemetite.

Again, the size classes used with the model should be chosen to give best results by having the greatest number of size classes possible, and choosing size classes to match feed and expected output size distribution.

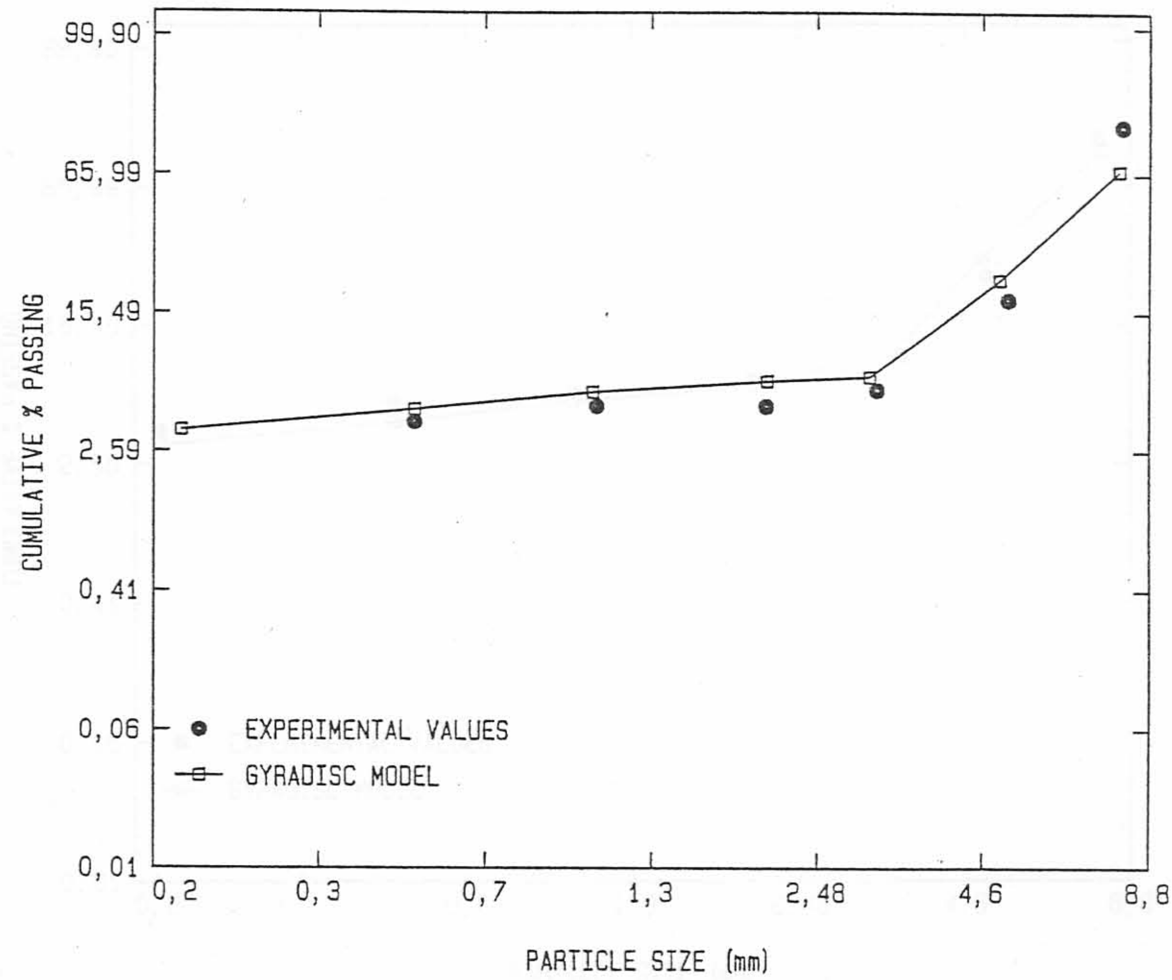

Fig 20 Rosin-Rammler plot for Gyradisc model output with closed side setting of 20mm, and experimental values

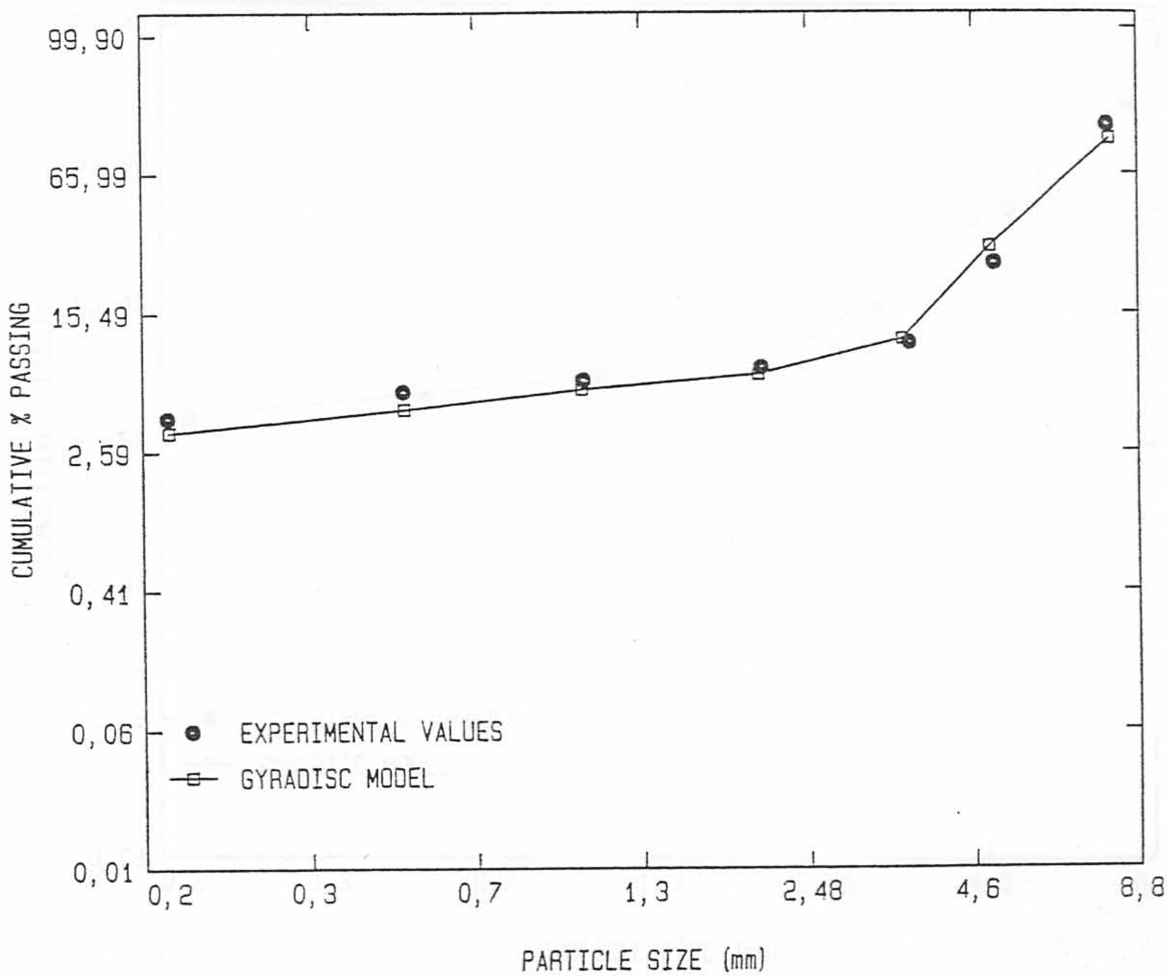

Fig 21 Rosin-Rammler plot for Gyradisc model output with closed side setting of 17mm, and experimental values

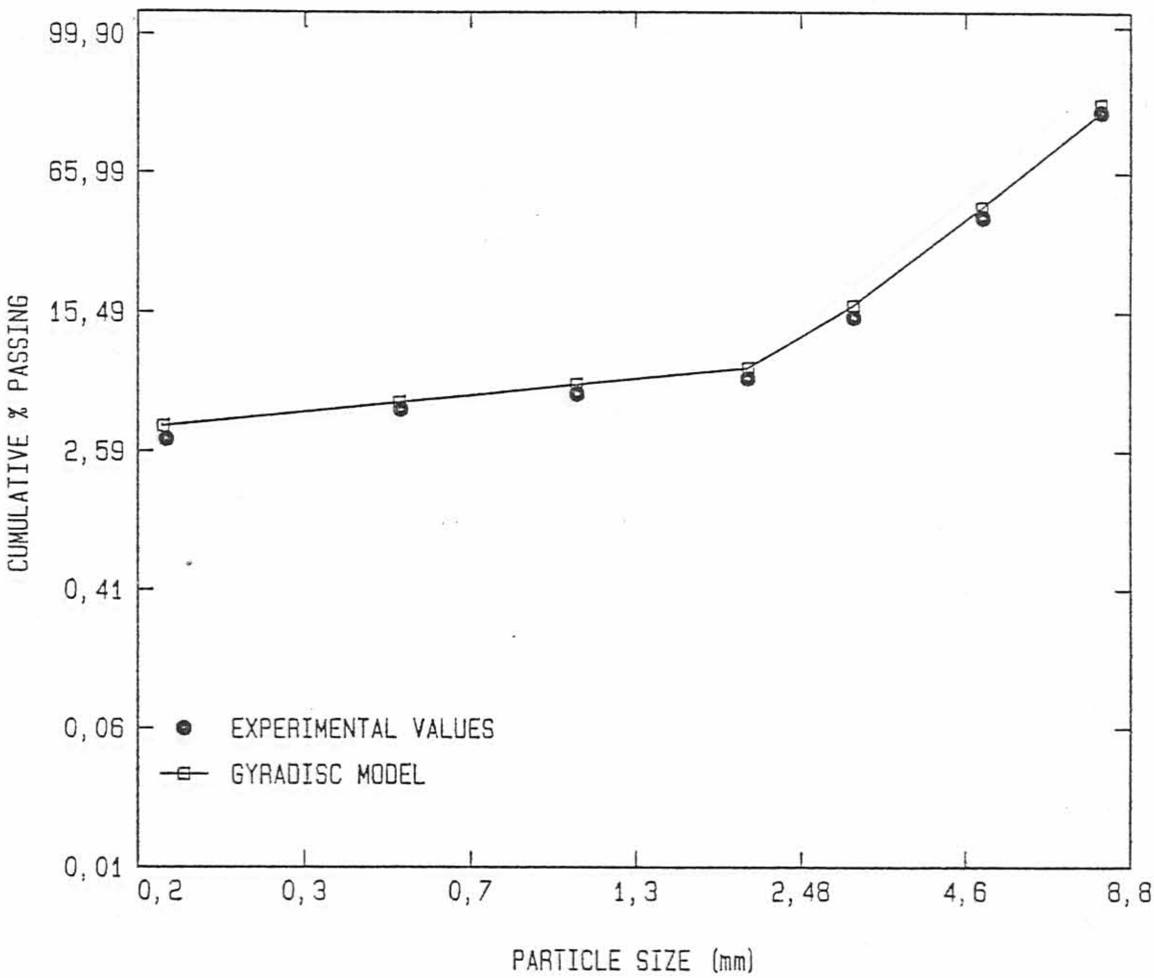

Fig 22 Rosin-Rammler plot for Gyradisc model output with closed side setting of 14mm, and experimental values

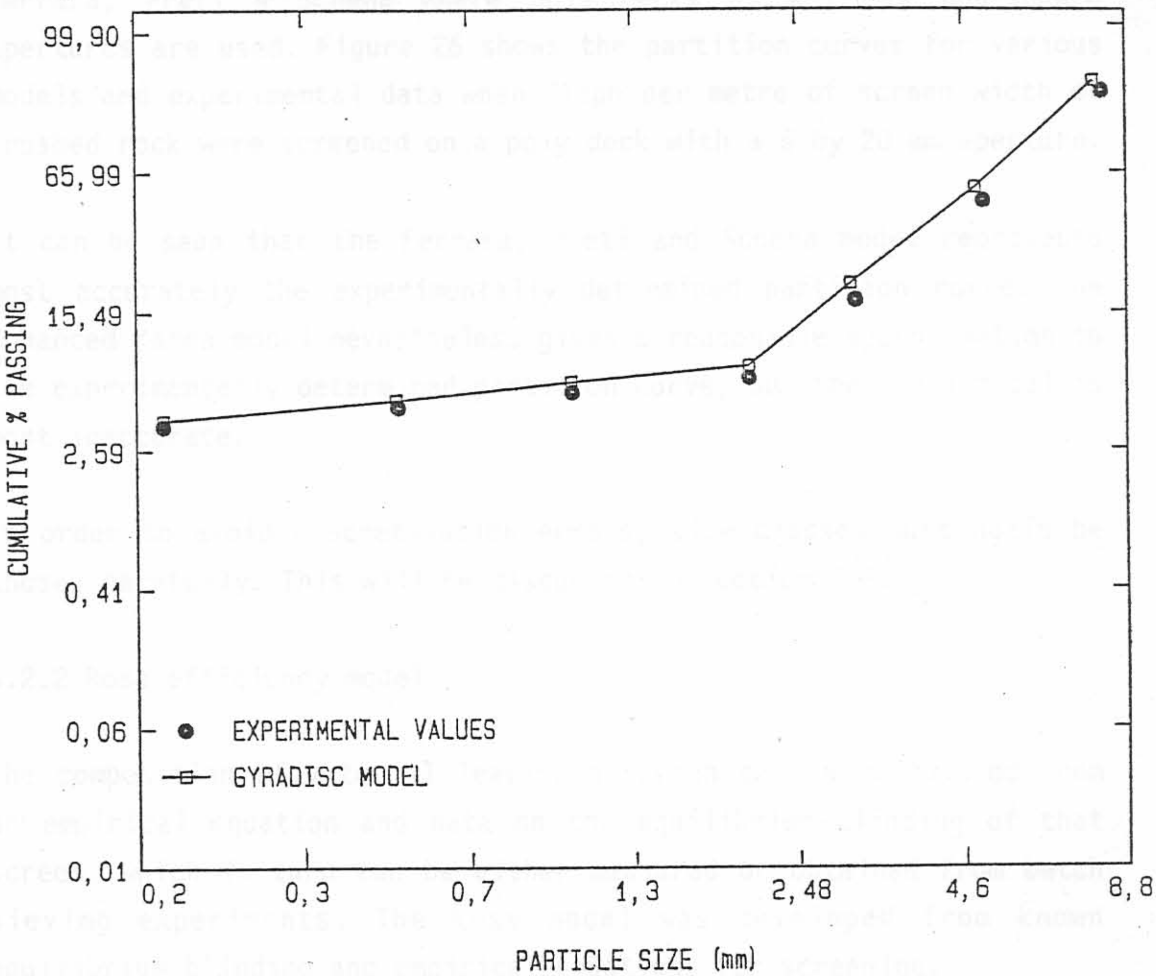

Fig 23 Rosin-Rammler plot for Gyradisc model output with closed side setting of 13mm, and experimental values

5.2 Screening models

Screening models were tested using the flow diagrams shown in figures 24 and 25.

5.2.1 Enhanced Karra model

This model was tested on a single deck using the test data of Ferrara, Preti & Schena (13) in order to compare the model to that of Ferrara, Preti & Schena where poly decks as well as non-square apertures are used. Figure 26 shows the partition curves for various models and experimental data when 71tph per metre of screen width of crushed rock were screened on a poly deck with a 6 by 20 mm aperture.

It can be seen that the Ferrara, Preti and Schena model represents most accurately the experimentally determined partition curve. The enhanced Karra model nevertheless gives a reasonable approximation to the experimentally determined partition curve, but the ideal model is most inaccurate.

In order to avoid discretisation errors, size classes must again be chosen carefully. This will be discussed in section 5.3.

5.2.2 Rose efficiency model

The composition of material leaving a screen can be calculated from an empirical equation and data on the equilibrium blinding of that screen, which in turn can be either measured or obtained from batch sieving experiments. The Rose model was developed from known equilibrium blinding and empirical equations for screening.

The single deck Rose model was tested against the Ferrara, Preti & Schena model and experimental data for a single screen with 4mm square apertures and at a feed rate of 60tph per metre of screen width and the partition curves are shown in figure 27, together with experimental values and the partition curve given by the ideal model.

It can be seen that the Rose efficiency model is almost as accurate as the Ferrara, Preti and Schena model in representing the experimentally determined partition curve, but that the ideal model is most inaccurate.

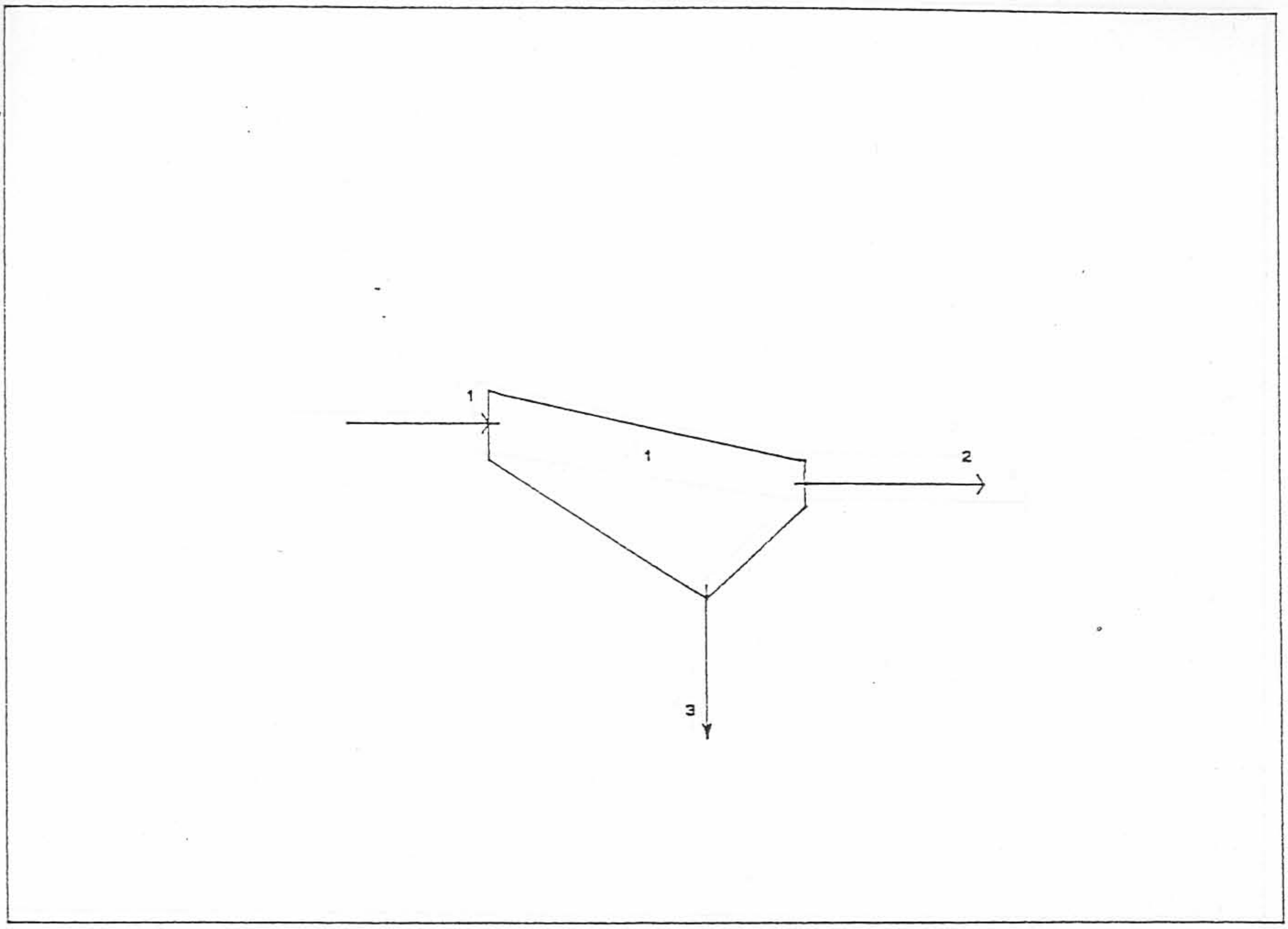

Fig 24 Flowsheet for testing single deck screen models

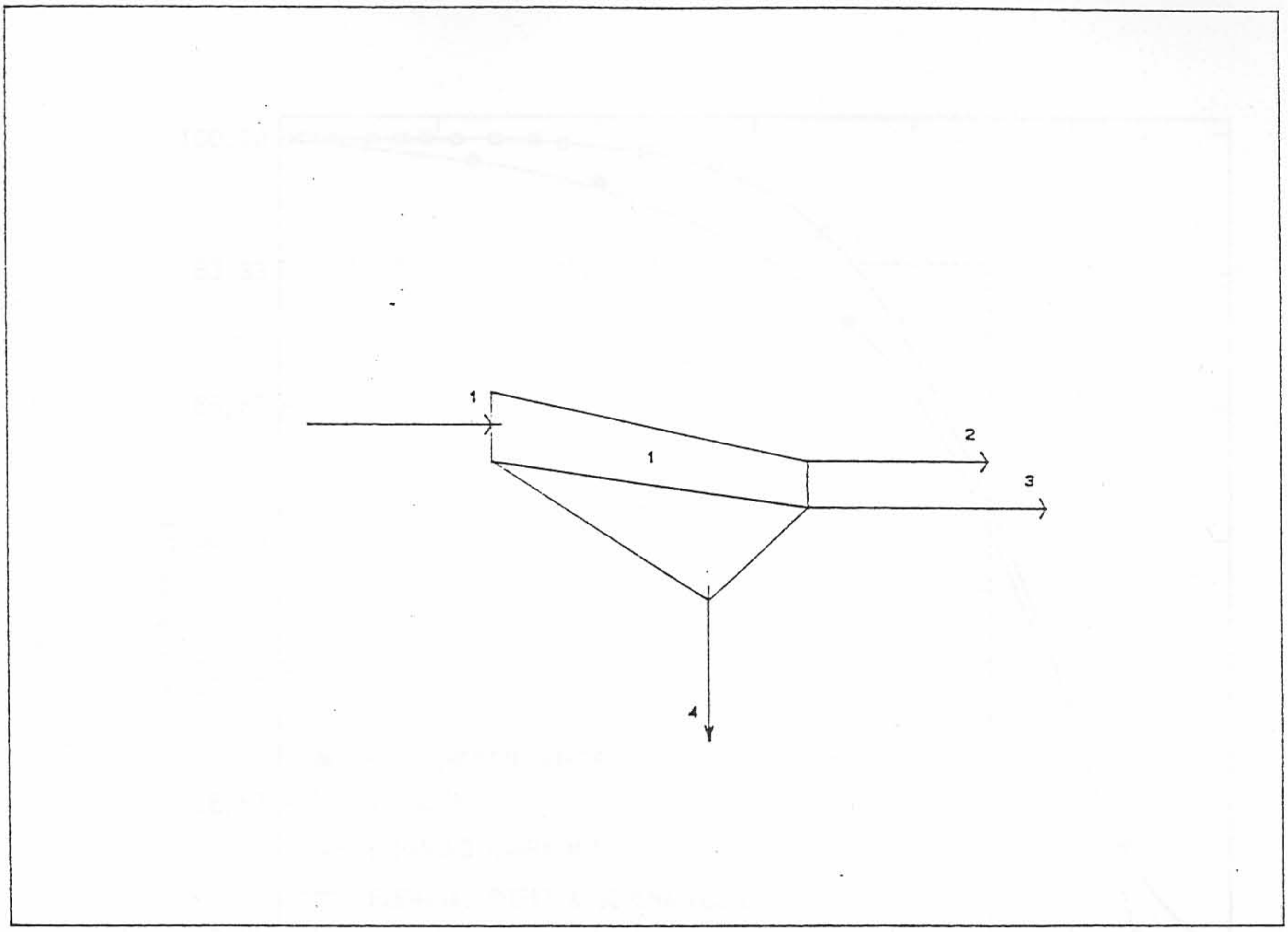

Fig 25 Flowsheet for testing double deck screen models

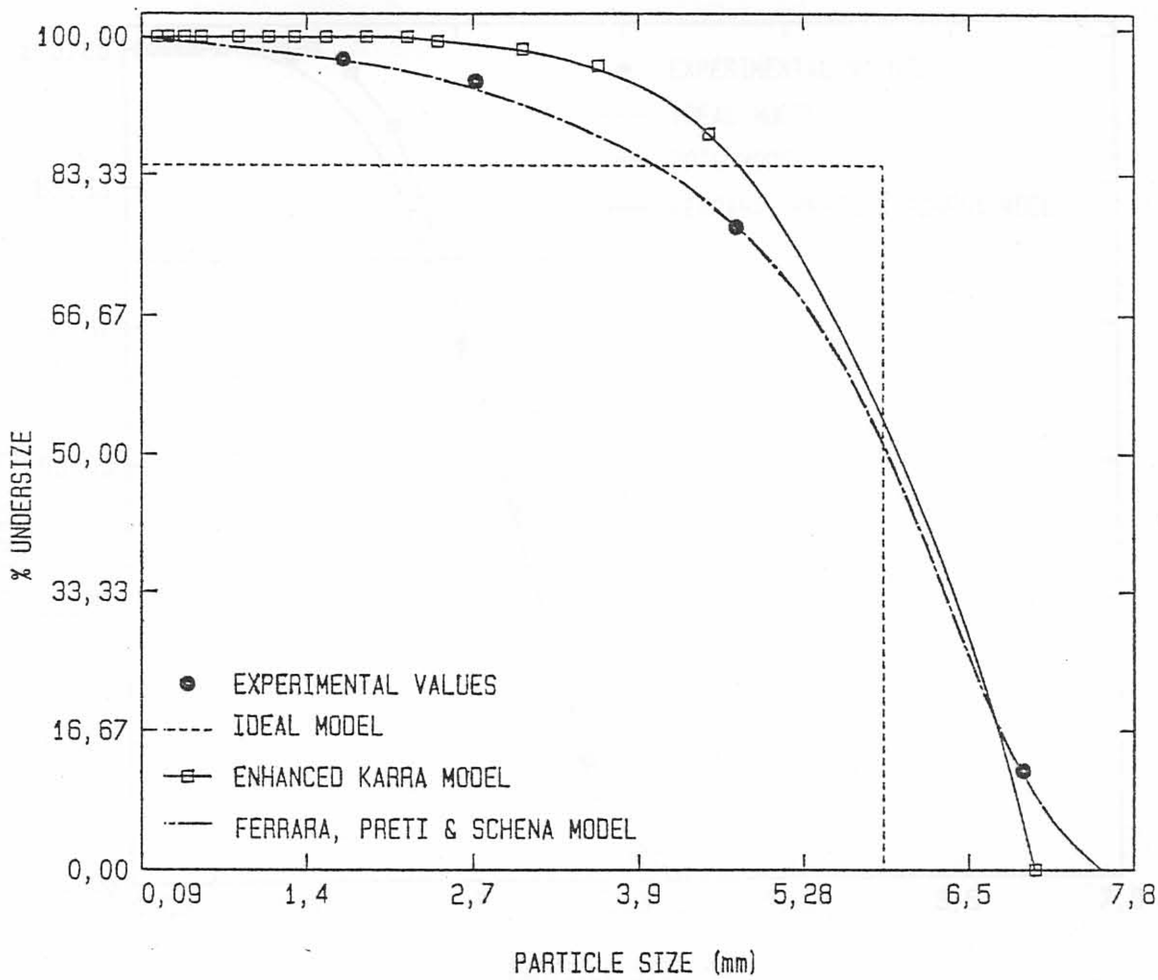

Fig 26 Partition curves for enhanced Karra & other models and experimental values, all for a single deck screen

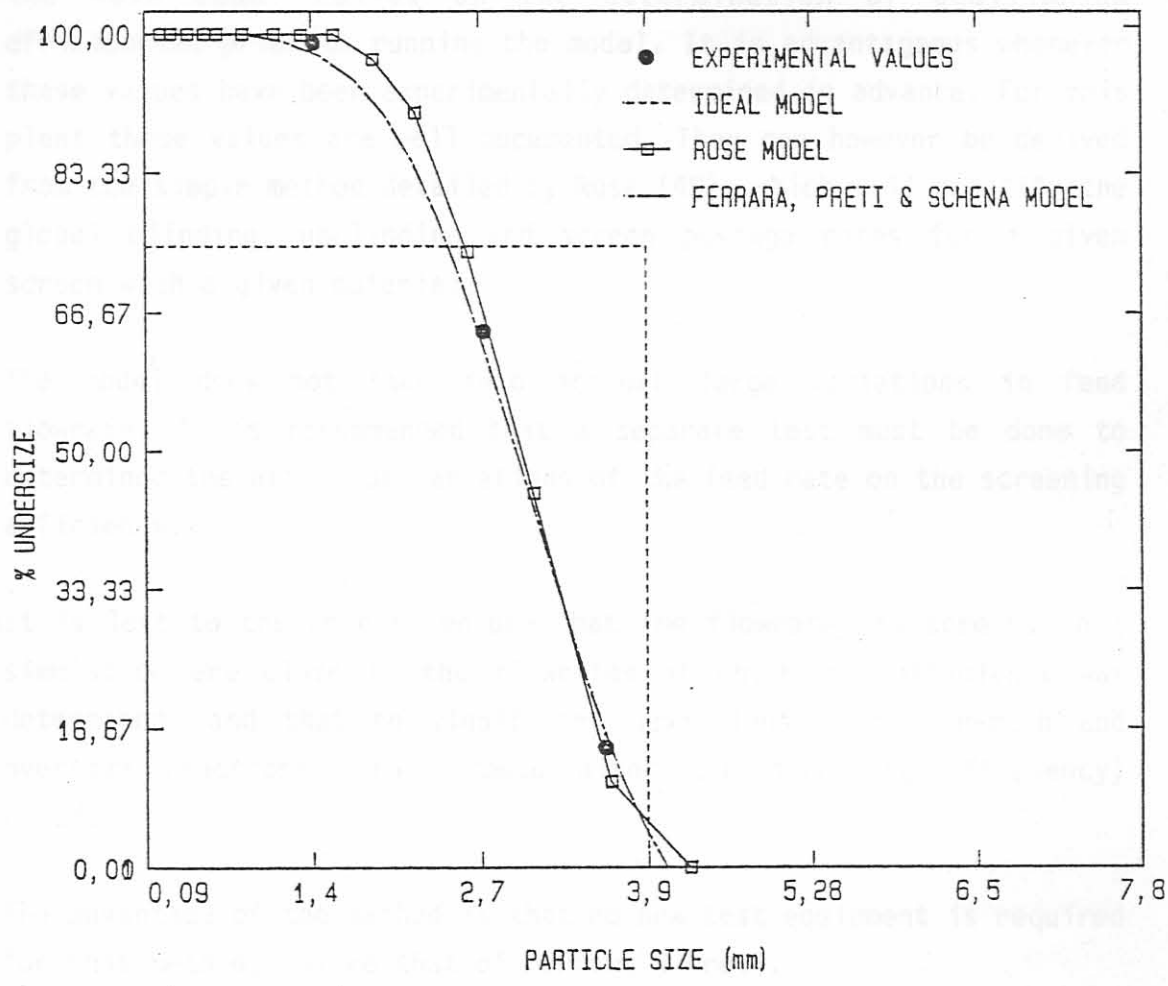

Fig 27 Partition curves for Rose and other models and experimental values, all for a single deck screen

By comparing figures 26 and 27 it can be seen that the Rose model gives better relative accuracy than the enhanced Karra model. This is not surprising as the enhanced Karra model relies entirely on empirically derived equations rather than measured values. The enhanced Karra model, however, can be used with no operating data. It is valid for most industrial processes and is thus completely transferable to other plants, where different screens are used and different materials screened.

The Rose model relies on the determination of equilibrium efficiencies prior to running the model. It is advantageous whenever these values have been experimentally determined in advance. For this plant these values are well documented. They can however be derived from the simple method detailed by Rose (49), which will quantify the global blinding, unblinding and screen passage rates for a given screen with a given material.

The model does not take into account large variations in feed flowrate. It is recommended that a separate test must be done to determined the effect of variations of the feed rate on the screening efficiency.

It is left to the user to ensure that the flowrates to screens in a simulation are close to the flowrates at which the efficiency was determined, and that no significant deviations from near-mesh and oversize fractions (which could alter the screening efficiency) occur.

The advantage of the method is that no new test equipment is required for this method, unlike that of Ferrara & Preti.

The model of Ferrara & Preti (13) uses the half-size mass velocity, k50 (described in section 3.4.3), to define the screening process by, effectively, one parameter for a given type of screen. This value is a strong function of aperture size, characteristics of the screening surface, vibration characteristics and inclination of the screen. As this model is the most accurate model, it would be helpful to build an empirical model around values of this parameter as specified by a given screen.

Sullivan's screenability characteristics method (52) can be used to apply this model to the screening of a new material with the same type of screens by determining a percentage change in screening efficiency. The Rose model can thus be used in a wide variety of plants and can even be used by a designer who has access to screening efficiency data of a manufacturer's screen and knows the screenability characteristics of his ore, to predict screening performance accurately. It is thus transferable to other plants.

5.3 Microsim and model accuracy

In this chapter, the flowsheets used for model validation (figures 17, 24 and 25) contain only one unit each. It is thus easy to choose size classes to fit the unit and to use the maximum number of size classes corresponding to the input experimental data, or the maximum number of size classes permitted by the simulator. This was set at 40 for Microsim, but Version 3.0 was restricted to 20 for use on a 640kB microcomputer. The user may change this by editing the file TYPEDEF.PAS and recomplililing the program.

The greater the number of size classes used, the better the discretisation of continuous functions by Microsim. It has been found that using too few size classes can sometimes lead to anomalous results.

For crushing applications, the effect of number of size classes is small, with more classes giving better approximations.

However, for screening applications, the choice of size classes is of utmost importance. To avoid anomalous results size classes should correspond to screen dimensions as closely as possible. This ensures that the representative size of the class is always on the same side of the screen aperture as the top size of the class.

When a partition curve is used there is another reason for choosing size classes carefully. The partition curve used by both the Karra and the Rose models is a steep function of size below mesh size, hence requiring small size classes to represent it accurately.

As an example, consider the double deck screen used for testing the screen models. Assume a user wished to ascertain how this double deck screen would perform if the top deck had an 8mm aperture size and the bottom deck a 5mm aperture size. However, the user has done a screen analysis of the feed stream and obtained the following input size classes: +10mm, -10/+5mm, -5/+3mm, -3/+2mm, -2mm, as these coincide with his laboratory equipment.

All the +10mm material will be assigned to the overflow of the top deck, as expected. However, the next size class has a representative size of 7,1mm, which is close to the screen aperture size. The partition coefficient corresponding to this representative size is close to unity (closer if the screening efficiency is low). This results in almost the entire -10/+5mm stream being assigned to the overflow of the top deck! The smaller fractions have low partition coefficients and hence pass almost completely to the second deck. Coefficients for the lower deck can then be calculated, whence a small amount of the -5/+3mm will be assigned to the overflow for the lower deck.

The simulator thus has assigned to the overflow of the bottom deck almost no material, with none of it in the -8/+5mm fraction.

When a far larger number of size classes were used, the overflow of the bottom deck contained more -8/+5mm particles, indicating that the error was due to the number of size classes chosen.

Size classes must be chosen with extreme care and with due consideration for the unit parameters in the flowsheet. If a flowsheet contains a large number of units, with a broad range of particle sizes being processed, it might be preferable to use the ideal screen model. This model has a step partition curve which is thus discretised without error. It is still useful to choose size classes with top sizes corresponding to screen apertures.

If Microsim is used to optimise screen apertures, of necessity, size classes cannot be chosen to coincide with screen apertures for each iteration of the optimisation routine. This can lead to anomalous results.

The question arises as to if and how one can extend limited experimental data to incorporate more size classes, i.e. how material in a large size class can be apportioned to a greater number of narrower size classes covering the original range. It was felt that the best way of accomplishing this was to plot the few experimental points on various axes to establish whether the data might fit a known size distribution (e.g. the Rosin-Rammler, Broadbent-Callcott, Gaudin-Melloy or Schumann). If so, then the appropriate distribution and its parameters could be entered into Microsim, and the user could then choose size classes to suit the flowsheet.

The above example and the model results illustrate that Microsim can provide accurate simulation of crushing and screening models, but the accuracy depends on the quality of information input to the simulator and the care taken by the user to avoid errors caused by discretisation.